©*Ibadan Journal of the Social Sciences*
Special Edition
Volume 23, No. 2, 2025
DOI: 10.36108/ijss/5202.32.0251

Drought Hazard Mapping and Groundwater Yield Enhancement through AI-driven Predictive Analytics and Geospatial Multi-criteria Evaluation

Josiah Ayomide Oluwaleye[1], John Faith Oyelakin[2], Deborah Ayodele-Olajire[3], Olalekan John Taiwo[4]
[1,2]Geographic Information System Unit, International Institute of Tropical Agriculture, Ibadan, Nigeria
[1,3,4]Department of Geography, University of Ibadan, Ibadan, Nigeria

The integration of Artificial Intelligence (AI) with Geospatial Multi-Criteria Evaluation is essential in data processing automation and in predicting future trends. This study investigates drought hazard and identifies groundwater yield zones in Nasarawa State, Nigeria. Nine hydrogeological factors were analysed spatially by utilising data derived from remote sensing and ancillary sources. The factors include a decadal 12-month Standardized Precipitation Index (SPI-12), Groundwater Storage Anomaly (GWSA), Rainfall, lithology, lineament density, drainage density, slope, aspect, and land use/land cover (LULC). Image processing and rose diagram generation, which depict lineament orientations, were performed using R and Python programming languages.The consistency ratio derived from the Analytical Hierarchy Process (AHP) was 0.0197, indicating that the assigned weights and the matrix were significant and coherent. The SPI-12 analysis for ten years revealed near-normal to mild drought conditions across the state, with the eastern region experiencing more pronounced dry periods. The local government areas most impacted by drought are Lafia and Awe, located in the eastern region of the study area.The application of an AHP established GWSA as the primary driver of groundwater yield with a weight of 38%. The AHP-generated map provided a generalized overview, which indicates a low yield in the eastern part and a high yield in the northern part. Artificial Intelligence (AI) was integrated to further enhance the groundwater yield AHP results; the result obtained revealed more detailed and nuanced patterns that AHP could not identify. Random Forest and Extreme Gradient Boosting (XGBoost) achieved accuracies of 99% and 98% respectively, which indicates their strong performance in predicting groundwater yield. The Precision-Recall and other graphs indicate the superior performance of Random Forest over XGBoost. The XGBoost performed well but showed a high false positive rate of 61% for moderate groundwater yield zones and missed an instance of high groundwater yield, unlike Random Forest. The models identified Keffi, Kokona, and others as high groundwater yield zones, while Toto, Awe, and others were classified as low groundwater yield zones.

Keywords: Drought, ground water yield, GeoAI, analytical hierarchy process, Geographic Information System, remote sensing

Introduction

Groundwater refers to water beneath the earth's surface within saturated zones, specifically in layers of sand, gravel, and pore spaces of crystalline and sedimentary rocks (Oseji & Ofomola, 2010). It exists in the voids within a geological stratum, making it a crucial natural resource for social development, especially in regions where water supplies are limited (Kordestani et al., 2019; Todd, 2004). Groundwater is stored in aquifer units and flows slowly across the subsurface geological formations (Idowu & Ojo, 2024). In crystalline Basement complex terrains, groundwater is located in fractured and weathered basement formations and partly in the transition zone between weathered and fresh basement rocks (Oni et al., 2020).Insufficient groundwater is among the drivers of drought globally (Rex et al., 2024).

Drought is a climatic condition that adversely affects ecosystems, water resources systems, and humans (Alam et al., 2013). It is a period of prolonged dryness or continuous shortage of water resulting from low rainfall or high temperature (Chen et al., 2009; Sordo-Ward et al, 2017). Drought is characterized by a temporary reduction in water availability over an extended period. The causes and consequences of drought are profound and have been documented in numerous studies (Orimoloye et al., 2021; Ayodele-Olajire, 2022). For instance, the western and southwestern regions of the United States (U.S.) have experienced severe drought events since the early 2000s, primarily due to below-normal precipitation (MacDonald, 2010; Ayodele-Olajire & Bolin, 2019). Some of the consequences of this was the triggering of 2015 widespread wildfires in the western U.S. and Alaska, scarcity of water resources, and low agriculture produce (Tanriverdi & Batmaz, 2025). Drought is complex and has more consequences than several other natural hazards, particularly in semi-arid to arid regions, due to their gradual onset and prolonged duration (Olabode et al., 2021; Tanriverdi & Batmaz, 2025). Consequently, these regions experience severe water shortages, making groundwater a necessary alternative (Fenta et al., 2015). Certain areas in the central and northern Nigeria face persistent drought problem, and attempts to access scarce groundwater has resulted in numerous borehole failures, largely due to inadequate prior information regarding the hydrogeological conditions of those areas (Ezekiel & Dominic, 2015; Alao et al., 2024).

Assessment of drought conditions in Nigeria has been conducted out using the Standardized Precipitation Index (SPI) and the Standardized Evapotranspiration Index (SEI) (Ogunjo et al., 2018; Ideki& Nwagbara, 2019; Obateru et al., 2023). Drought indices are always used to determine droughts, and the derived information from these drought indices is used for designing applications and planning (Sordo-Ward et al., 2017). According to Adeaga (2010), the Sahel savannah in Northern Nigeria is prone to extreme drought, while the Sudan and Guinea savannahs usually experience mild to moderate drought. In the central part of Nigeria, drought vulnerability assessment was carried out by Ideki and Nwagbara (2019) using SPI and geospatial techniques. The results indicate increasing trends of drought with near normal to moderate conditions in Abuja, Ilorin, Lafia, and Lokoja; and moderate to severe droughts in Minna and Jos. Obateru et al. (2023) assessed drought conditions and rainfall trends in southwestern Nigeria using 1984-2014 rainfall dataset. Their results largely showed a cyclical SPI pattern and indicated Ibadan and Oshogbo as the driest and wettest stations, respectively. These findings highlight the need for drought monitoring as a water management strategy.

Groundwater is a dynamic resource influenced by various environmental factors, including drought, drainage patterns, land use and land cover (LULC), geomorphology, lithology, topography, slope, precipitation, soil characteristics, and hydrological conditions (Pradhan 2009). Unlike surface water, groundwater is less susceptible to pollution; rather, it is significantly affected by underlying geology, the intensity of chemical weathering, recharge efficiency, groundwater levels, and the origins of certain surface elements (Yıldırım 2021). The demand for groundwater in North Central Nigeria is increasing due to the combined effects of drought, rapid population growth, and urbanization (Ezekiel & Dominic, 2015).

The integration of Artificial Intelligence (AI), Remote Sensing (RS), and Geographic Information System (GIS) tools presents a cost-effective, efficient, and robust approach to mapping groundwater yield zones (Manap et al., 2014; Gerlach et al., 2022). The use of RS, geospatial modeling, and AI in hydrologic studies varies based on the specific question being asked, the scale of the study in terms of space and time, and the type, amount, and quality of the data available (Gerlach et al., 2022; Ayodele-Olajire & Olusola, 2022). Nevertheless, these tools excel in managing extensive and complex datasets while providing insights across various spatial and temporal dimensions (Jha et al., 2007; Singh et al., 2019; Afan et al., 2021). The use of GIS and Remote Sensing, in conjunction with the Analytic Hierarchy Process (AHP), proves beneficial for investigating groundwater yield zones across diverse geological contexts and demonstrates effectiveness in defining these zones (Thapa et al., 2017; Igwe et al., 2020). Many studies have integrated different factors like geology, landforms, lineament density, drainage density, and slope in a GIS environment to find groundwater potential zones (Morea & Samanta, 2020; Ahmed et al., 2021; Ajayi et al., 2022). Deciding how much weight to give each factor is often based on expert opinions or reviews of existing research, which can be somewhat subjective (Ahmed et al., 2021) and may yield incorrect results (Adesola et al., 2023).

The AHP method coupled with GIS is used in identifying zones with groundwater potential by examining how these factors interact with each other. However, there is a lack of comparison between AHP and AI groundwater potential results, which can be useful in examining the accuracy and dependability of AHP results. When addressing decision-making cases, AHP aids in the representation of problems by integrating several criteria, while an order of importance is established within the structure by pairwise comparison. Nevertheless, AHP can exhibit inconsistencies in its measurements and dependencies among element groups (Ajayi et al., 2022). Thus, employing AI in identifying groundwater recharge zones, and then comparing these results with traditional AHP results helps to eliminate expert bias, capture non-linear relationships, and ensure model reliability.

Machine learning algorithms, a subset of AI, have recently evolved in precise forecast modeling, identifying detailed patterns, particularly irregular data, and developing extremely accurate forecast models (Olden et al., 2008). AI can detect subtle patterns that may not be accurately detectable in traditional methods. They have a more substantial mastery of resolving complicated interactions due to their advanced learning and decision-making capabilities (Zaresefat et al., 2022). This study aims to assess the spatio-temporal patterns of drought hazard and delineate groundwater yield zones in Nasarawa State, Nigeria, by comparing Artificial Intelligence and Analytical Hierarchy Process methods for robust decision-making.

Materials and Methods

Study Area

The study area, located in Nasarawa State in North Central Nigeria between Longitude 6°32ˈ30ˈˈE to 9°34ˈ0ˈˈE and Latitude 7°48ˈ30ˈˈN to 9°49ˈ30ˈˈN, with a total area of approximately 27,117 km² (Figure 1). This region is situated within the middle Benue Trough, which refers to the central portion of Nigeria's Benue Trough. Nasarawa State is bordered by Benue State to the south, Kaduna State to the north, Taraba State to the east, and Abuja to the west. Geological analysis indicates that about 60% of the area is characterized by Basement complex rocks, while the remaining 40% comprises sedimentary rocks associated with the Benue Trough (Adewumi & Salako, 2017). The climate of the research area is predominantly warm tropical, featuring relatively high temperatures year-round, with an average monthly temperature around 27.5°C; maximum daytime temperatures can vary between 25 to 30°C, depending on seasonal changes (Iloeje, 1981). The seasonal weather pattern is marked by a prolonged wet season from late March to July, interspersed with intense rainfall, a brief dry season from late July to August, followed by a short-wet season in September and October, before the onset of the dry season in November (Iloeje, 1981; Ifediegwu, 2022).

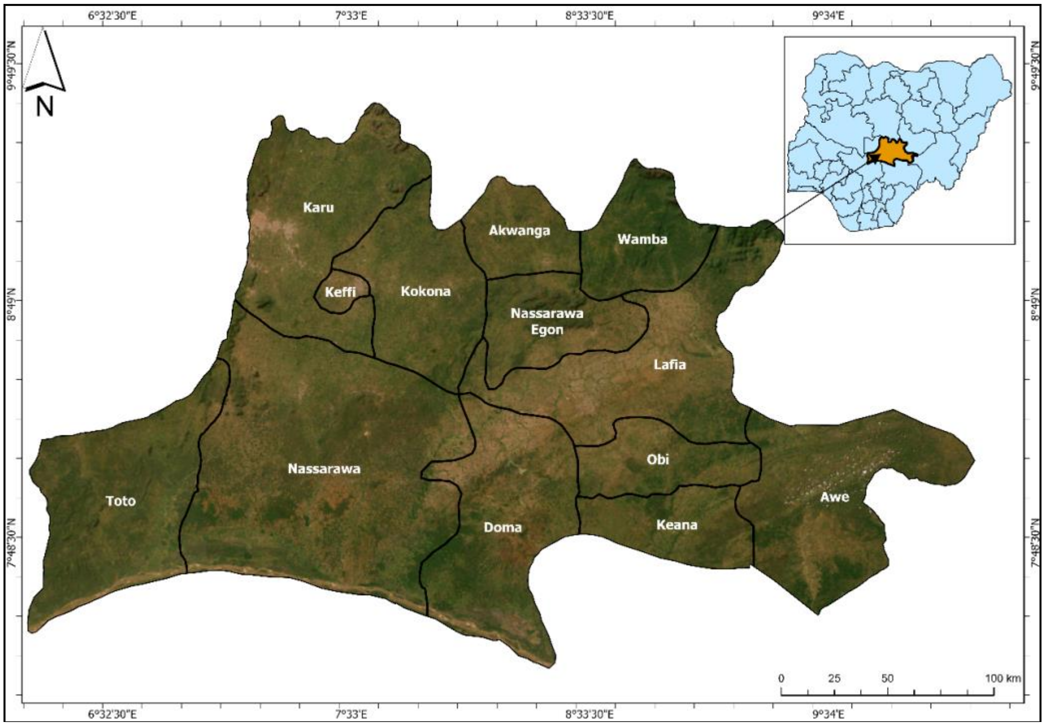

Figure 1: Map of Nasarawa State showing the Local Government Area sand its location within Nigeria

Preparation of the Thematic Areas

The Landsat 8 imagery for December 27, 2024, and the Digital Elevation Model (DEM) were both obtained from the USGS Earth Explorer portal (www.earthexplorer.usgs.gov). Additionally, lithology data and population settlement data were sourced from the ESRI and GRID3 websites, respectively. For the AI and AHP models, nine thematic layers were analyzed, including Groundwater Storage Anomaly (GWSA), Rainfall, Standard Precipitation Index (SPI), lineament density, drainage density, slope, aspect, Land Use Land Cover (LULC), and lithology datasets.

Lineaments were generated through the manual digitization of a hillshade dataset derived from Landsat data, focusing only on those of enough size to minimize noise and prevent the introduction of spurious features (Ajayi et al., 2022). The length of each lineament, along with its coordinate endpoints (X and Y), was calculated within ArcGIS Pro. Additionally, a rose diagram illustrating the orientation of these lineaments was created using the Python programming language, and a line density analysis was performed to derive the Lineament density per square kilometer.

The fill function was applied to the Digital Elevation Model (DEM) data to address sinks and peaks, effectively correcting minor imperfections in the raster data (Ajayi et al., 2022; Boitt et al., 2023). Following this, a flow direction map was constructed utilizing the D8 method available in the hydrology toolset of ArcToolbox, which was executed on the filled raster. The flow accumulation was then derived from the flow direction output. Stream order analysis was subsequently conducted using both the flow direction and accumulation results. This analysis led to the stream to feature assessment based on the “stream order” output. To visualize the results, the stream to feature data was converted to graduated symbols in Symbology, with grid code selected as the associated value. Finally, a line density analysis was performed on the stream to feature results to determine the drainage density, while the slope and aspect layers were extracted by applying the respective tools to the DEM data within ArcGIS Pro.

A composite raster was generated by utilizing Blue, Green, Red, Near-Infrared (NIR), Shortwave Infrared (SWIR) 1, Thermal, and SWIR 2 bands from the Landsat imagery. For the supervised classification process, the selected band combination consisted of NIR, SWIR, and Red. In this classification, built-up regions were represented in shades ranging from white to grey, while open spaces exhibited various tones of brown. Water-covered areas were depicted in bluish or blackish hues, and vegetative regions appeared green. Training samples for the four classes, including built-up areas, open spaces, water bodies or wetlands, and vegetation zones, were digitised from the composite raster and verified using Google base map. The number of samples for each category ranged from 74 to 170. These training samples were employed to extract pixel values from the composite image utilizing the R programming language. Finally, the Random Forest (RF) and Support Vector Machine (SVM) algorithms were implemented in Python to generate the Land Use Land Cover (LULC) map, achieving an overall accuracy of 80% and 82% respectively. The SVM result was used as the LULC layer for further analysis due to its better accuracy. Additionally, the lithology layer for the region was sourced from ESRI, with a resolution resampled to 30 meters to align with the resolution of the other raster data layers.

The launch of the Gravity Recovery and Climate Experiment (GRACE) satellites in March 2002 made it possible to assess and analyze groundwater storage (Rodell & Reager, 2023). The Groundwater Storage Anomaly (GWSA) was estimated using equation i.

$$GWSA = TWSA - SMSA - SWSA - SWEA - CWSA \quad \text{.. equation i}$$

Where TWSA-total water storage anomaly, SMSA-soil moisture surface anomaly, SWEA-surface water storage anomaly, and CWSA-canopy water storage anomaly (Ma et al., 2024). Google Earth Engine (GEE) was used to analyze storage rasters and generate the final mean GWSA output from January 2024 to December 2024.

Rainfall and Standard Precipitation Index

This study used geospatial data techniques and the Python programming language to obtain the mean rainfall layer and to calculate long-term drought impact using a 12-month standard precipitation Index (SPI-12) for ten years (January 2014 – December 2023). The monthly time series rainfall data were downloaded from the Climate Hazards Group InfraRed Precipitation with Station data (CHIRPS) website (https://data.chc.ucsb.edu/products/CHIRPS/v3.0/monthly/africa/). The mean rainfall raster for the 10 years was calculated and represents the rainfall layer used for further analysis. To obtain the SPI layer, each monthly raster dataset was read, and negative values were masked to avoid bias during calculation. After which the rainfall raster data were stacked into a 3-dimensional array using the NumPy library in Python. For each pixel, the sum of rainfall and accumulated rainfall fitted with a gamma distribution was calculated for 12 months to compute SPI-12 (Svoboda et al., 2012). The study used a gamma distribution, which is a function of probability density, to fit the long-term rainfall data as described by Ogunrinde (2018). Extreme wet and dry conditions were identified by SPI values greater than 2 and less than -2, respectively (Table 1) (Bordi et al., 2007).

Table 1: Weather Classification according to SPI Values

SPI values	Classification
2.00 and above	Extremely wet
1.50 – 1.99	Very wet
1.00 – 1.49	Moderately wet
-0.99 – 0.99	Near Normal
-1.00 - -1.49	Moderately dry
-1.5 - -1.99	Severely dry
-2.00 - less	Extremely dry

Analytical Hierarchy Process (AHP) Modeling

The Analytical Hierarchy Process (AHP), introduced by Saaty in 1980, is frequently referred to as the Saaty method (Saaty, 1980; Saaty, 1990; Wang et al., 2008). This approach is a qualitative traditional method that has been utilized in the analysis of multi-criteria decision-making problems to derive solutions with greater accuracy. By employing pairwise comparisons, AHP facilitates the calculation of the relative importance of various attributes, yielding a significance test for the features under consideration (Wang et al., 2008).

The ranks for the nine thematic layers were assigned based on Satty's scale (Table 2) with expert knowledge based on the influence of each layer on groundwater occurrence using the AHP technique. To calculate the consistency vector (λ), the pair-wise comparison matrix values were multiplied by normalized pair-wise matrix values of the thematic layers using matrix multiplication (Muralitharan and Palanivel, 2015).

$\lambda = \Sigma(C_{ij}X_{ij})$ where λ= Consistency vector. Consistency Index (CI) was calculated using the following formula:

$CI = \frac{\lambda - n}{n-1}$… equation ii

where *CI* = Consistency Index, n = Number of criteria used, RI= Random Consistency Index for 9 variables (Table 3). Consistency Ratio (CR) was calculated using the following formula:

$CR = \frac{CI}{RI}$… equation iii

A consistency ratio of <0.1 means the assigned weights and the matrix were significant and coherent (Saaty, 1990). All the thematic layers were reclassified using the ArcGIS Pro. Finally, the groundwater yield zones were identified by integrating all the thematic layers using the weighted overlay technique in the spatial analysis tool. The result was classified into three classes, namely: high, medium, and low groundwater yield zones

Table 2: Saaty's 1-9 Scale of Pairwise Comparison Importance (Saaty, 1990)

Intensity of Importance	Definition
1	Equal important
3	Somewhat more important
5	Much more important
7	Very much more important
9	Absolutely more important
2, 4, 6, 8	Intermediate values when a compromise is needed

Table 3: Saaty's ratio index for different values of n (Saaty, 1990)

Order	1	2	3	4	5	6	7	8	9	10
RI	0	0	0.52	0.89	1.11	1.25	1.35	1.4	1.45	1.49

Artificial Intelligence (Machine Learning) Modeling

Locations of known groundwater (borehole and hand-dug wells) in Nasarawa were obtained from previous studies (Kana et al., 2014; Obaje et al., 2020; Cardiff University, n.d.). A total of 70 Training samples were extracted from these locations. An established protocol for sourcing training samples in regions with sparse in situ data was followed (Nishimura et al., 2022). Groundwater yield zones were categorized into three classes based on borehole clustering density as well as GWSA and SPI results. Clustered borehole points were labelled as "High Yield", the non-clustered ones and hand-dug well locations were labelled as "Moderate Yield", while areas with very low groundwater accumulation and areas highly affected by drought were labelled as "Low Yield" using the GWSA and SPI layers. R programming was used for pixel extraction, while Python was used for other preprocessing and modeling. A total of 362 training samples were obtained after pixel extraction from all nine layers. The nine layers and the shapefile were projected to UTM Zone 32N for area-based analysis. A 30-meter spatial resolution was adopted, layers were stacked into a multi-band array, and pixels containing no data were identified and excluded from the modelling. The training data was split into 70% and 30% for training and testing, respectively. Random Forest and Extreme Gradient Boosting (XGBoost) algorithms were trained using 100 estimators. The models were evaluated based on an independent testing set. Overall accuracy, feature importance (as bar charts), confusion matrix, classification result, and the final raster outputs were generated from the algorithms.

Results

Slope and Aspect Thematic Layers

In the study area, slope values range from 0° to 74°, with the majority of steep slopes located in the northern region (Figure 2a). Furthermore, the overall topography indicates a prevailing inclination towards the northern and eastern aspects (Figure 2b).

Lineament and Lineament Density Thematic Layer

Hillshade raster was used to effectively extract lineaments, due to its ability to enhance topographic expressions (Figure 2c). Python programming generated a Rose diagram of the study area, indicating that the predominant orientations of the lineaments are directed toward the northeastern sector (Figure 2d). The lineament density values observed in the study area range from 0 to 134 km/km², with the highest densities, between 19 and 134 km/km², predominantly located in the southern and central regions (Figure 2e).

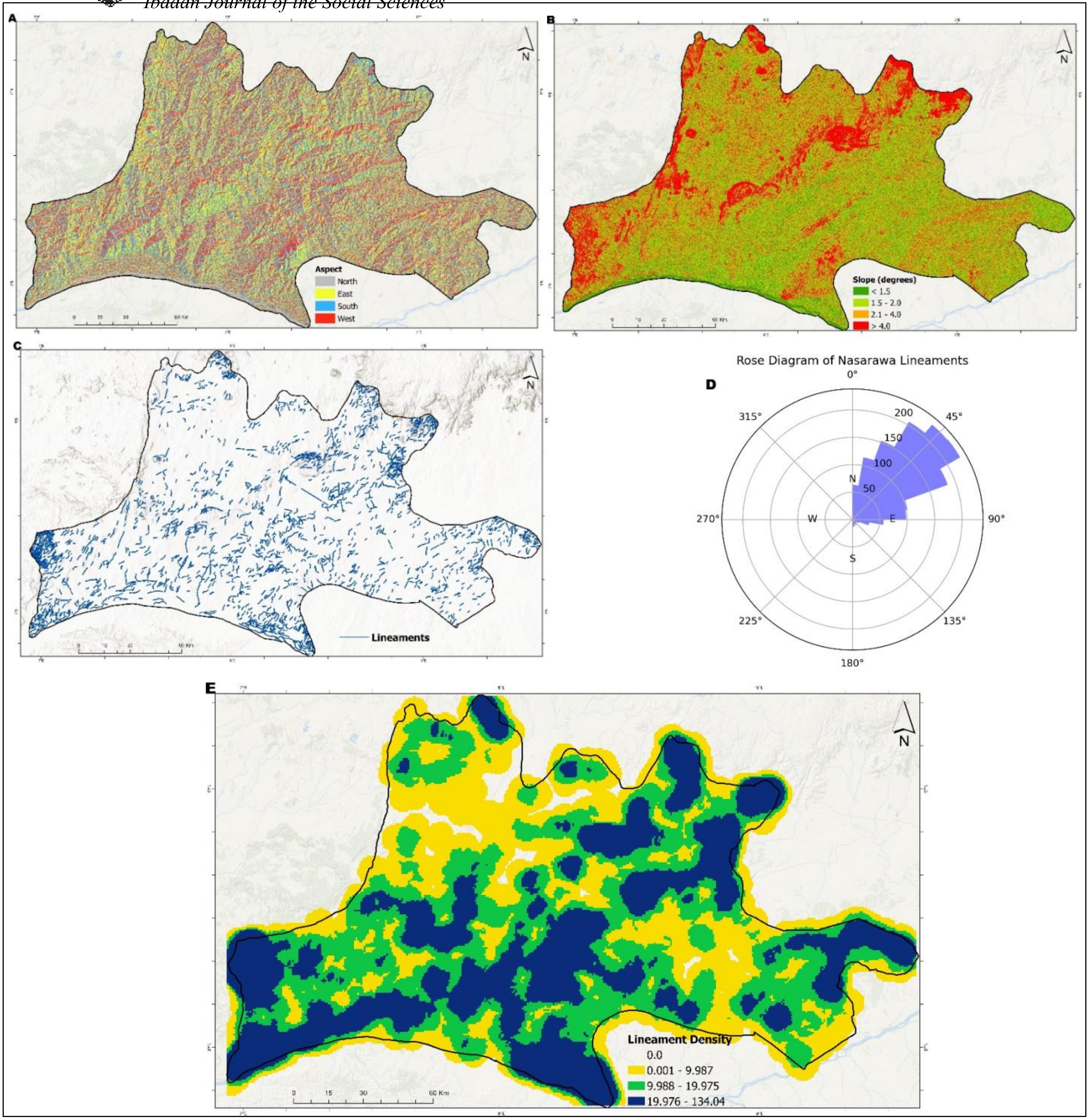

Figure 2(a): Aspect map showing the orientation of the slope. (b)Slope map showing the level of steepness. (c)Manually digitized lineaments of the study area. (d)Rose diagram showing the orientation of the lineaments to the NE of the study area. (e)Lineament density showing zones of high and low densities

Lithology and Land Use Land Cover Thematic Layers

In the study area, four distinct lithologies have been identified: unconsolidated sediment, siliciclastic sedimentary rock, acid plutonics, and metamorphic rocks (Figure 3a). Unconsolidated sediments, such as gravel, sand, and silt, are characterised by high porosity and permeability, enabling efficient water movement. Siliciclastic sedimentary rocks, which originate from the fragmentation of pre-existing rocks, include porous and permeable varieties such as sandstone, shale, and siltstone. Conversely, acid plutonics, exemplified by granite, and metamorphics, represented by gneiss, typically exhibit lower porosity and permeability; however, highly fractured metamorphics can develop secondary porosity and permeability enhancements.

Land use and land cover encompass both natural and anthropogenic features present on the Earth's surface. In the study area, open space categories are the most dominant (41.87%), followed by water bodies and wetlands (34.59%), vegetation (12.87%), and urbanized regions (10.67%) (Figure 3b). Settlement areas are primarily located in the northwestern and eastern sections of the study area. Additionally, water bodies and wetlands are prevalent in the southern region of Nasarawa, which aligns with the course of the Benue River and the various smaller rivers feeding into it from different areas.

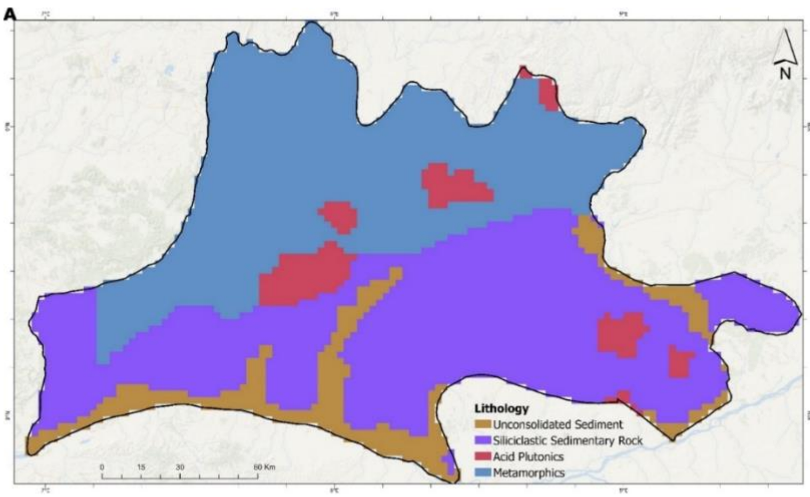

Figure 3a: Lithology map showing the rock types that are peculiar to different parts of the study area

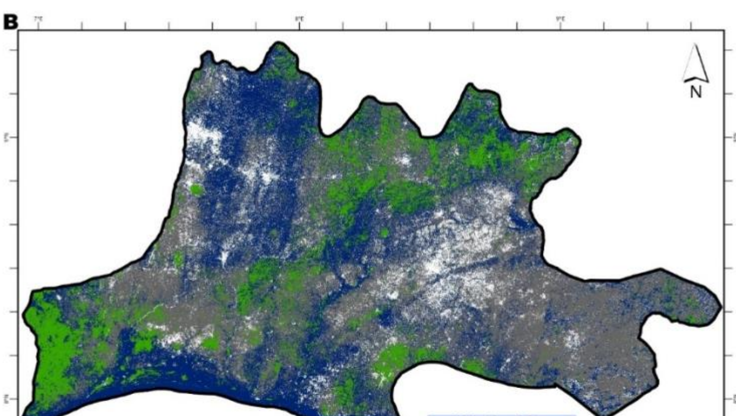

Figure 3b: LULC map derived from support vector machine showing predominance of open spaces, followed by water bodies and wetlands, vegetation, and built-up land use

Standard Precipitation Index and Drainage Density Thematic Layers

In the study area, a notably high drainage density pattern extends from the northern and western regions towards the southern area, where the Benue

River flows. Noteworthy rivers in Nasarawa State include the River Mada, River Dep, River Inaji, River Ahina, and River Farin Ruwa. Rivers Mada and Dep primarily traverse from the central region to the south, while River Farin Ruwa descends from the southwestern area. In contrast, Rivers Inaji and Ahina originate from the southeastern sector of the study area. The majority of regions exhibiting the highest drainage density levels are located in the southern and central parts, with recorded values exceeding 4550 km/km² (Figure 4a). For groundwater assessment, it is observed that lower drainage density corresponds to higher infiltration rates (Lavanya & Muthukumar, 2024). Consequently, lower-density drainage is assigned a higher rank, while higher-density drainage receives a lower rank.

The SPI result generally shows that the drought impact in Nasarawa over the ten years is near normal or mild (between 0 to -0.99) (Figure 4b). Locations with positive SPI values occur in the northwestern and the southern regions of the study area, which indicates greater than median precipitation or wet conditions. Most of the areas with negative SPI values are in the eastern part and a few in the south western part of the study area, indicating less than median precipitation or dry conditions (drought).

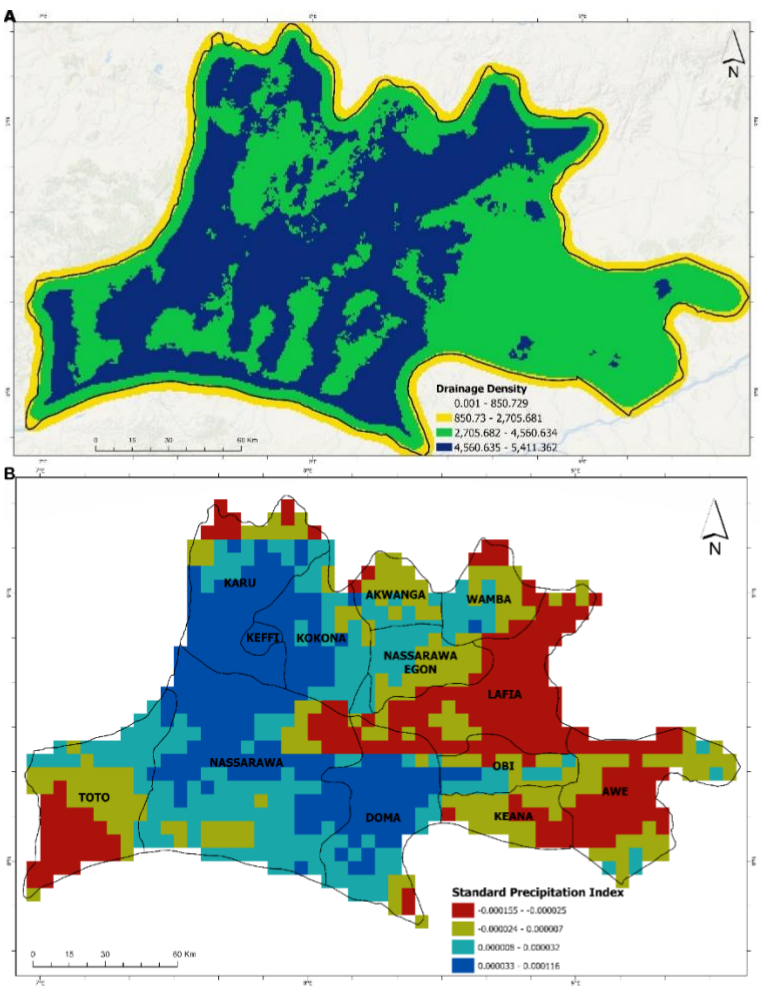

Figure 4: (a) Drainage density map showing low and high zones of drainage in the study area. (b) SPI map showing dry and wet areas of the study area

Rainfall and Groundwater Storage Anomaly

The result obtained for the mean rainfall layer is presented in Figure 5. Areas that recorded high rainfall over the past decade are in the northern and central parts. Some parts of the eastern side and most of the southern part of the study area recorded lower rainfall.

Similarly, the GWSA result in Figure 6 shows that most of the northern part of the study area, particularly the northeastern part, has high groundwater accumulation. Although the negative values suggest that in 2024, Nasarawa State faced a challenge with declining groundwater levels. The central and southern parts have a moderate groundwater accumulation, while the eastern part has a low groundwater accumulation. The low groundwater accumulation recorded for the eastern parts corroborates the rainfall and SPI results. Likewise, the high groundwater accumulation in the northeastern part corroborates the Rose diagram results, which indicates that the lineaments are oriented towards the northeastern part of the study area.

Rainfall and Groundwater Storage Anomaly

The Analytic Hierarchy Process (AHP) was employed to ascertain the relative importance of each criterion, as detailed in section 3.1. The scale of importance assigned to each criterion and the calculated normalised weights are presented in Tables 4 and 5. These criteria were subsequently integrated using the weighted overlay tool within the ArcGIS environment to generate the groundwater yield zones map for the study area. The weights determined through AHP calculations were: 4% for land use/land cover (LULC), 4% for slope, 4% for lithology, 4% for aspect, 4% for drainage density, 7% for the Standard Precipitation Index (SPI), 11% for lineament density, 24% for rainfall, and 38% for GWSA (Figure 7). The calculated consistency index (CI) was 0.0286, and using a random consistency index of 1.45 for the nine variables, the resulting consistency ratio was found to be 0.0197, indicating that the assigned weights and the matrix were both significant and coherent.

The analysis of the weighted overlay output indicates that the study area generally has a moderate groundwater yield. Most of the northern region and some parts of the central region exhibit high groundwater yield. In contrast, a considerable portion of the eastern region is characterised by low groundwater yield. An overlay of population points reveals settlements that correspond to the varying groundwater yield zones. Specifically, Local Government Areas (LGAs) that fall within the low groundwater yield zones include Awe and minor parts of Lafia (e.g., Arikya locality), Doma (e.g., Akpanaja locality), and Nasarawa (e.g., Loko locality) (Figure 8). Furthermore, the high groundwater yield zones are Nasarawa Egon, Akwanga, Karu, Wamba, Lafia, and some parts of Obi, Keana, Kokona, Nasara, and Doma.

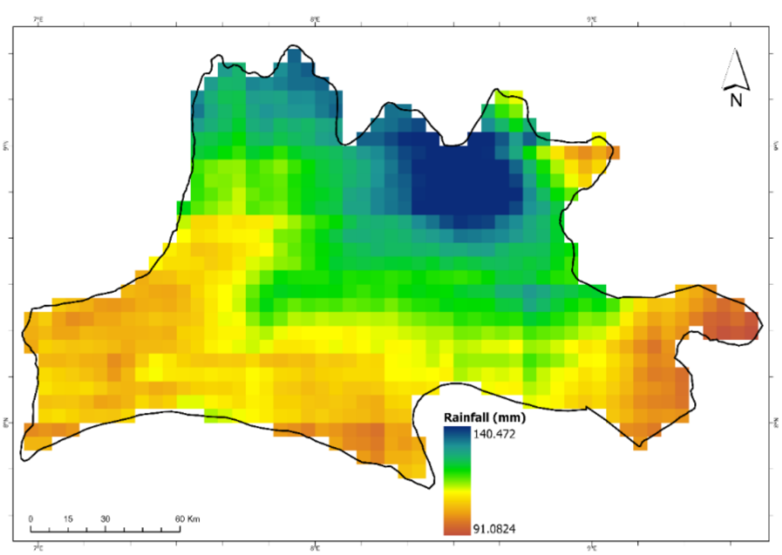

Figure 5: Average rainfall from 2014-2024 showing high and low rainfall patterns in the study area

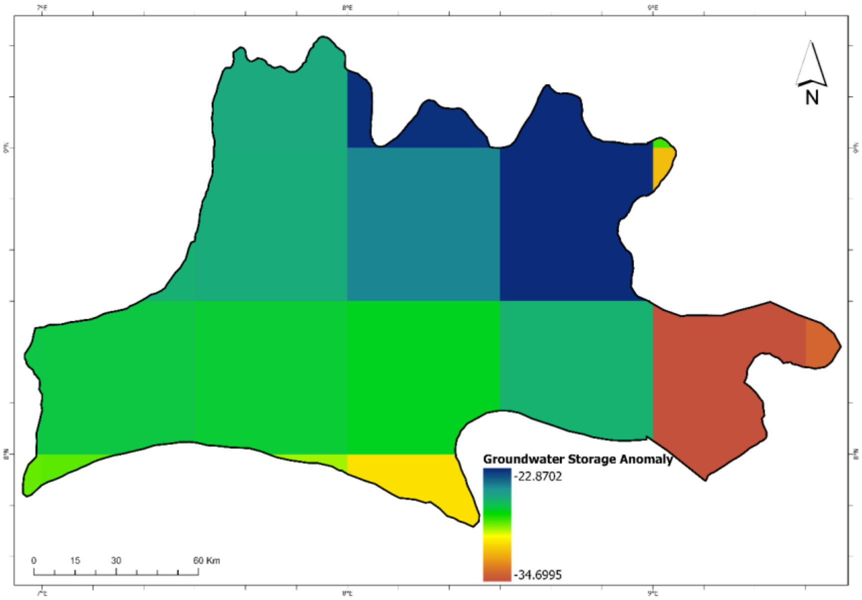

Figure 6: GWSA map showing patterns of groundwater accumulation (storage) in the study area

Analytical Hierarchy Process (AHP) and Weighted Overlay Tool

The Analytic Hierarchy Process (AHP) was employed to ascertain the relative importance of each criterion, as detailed in section 3.1. The scale of importance assigned to each criterion and the calculated normalised weights are presented in Tables 4 and 5. These criteria were subsequently integrated using the weighted overlay tool within the ArcGIS environment to generate the groundwater yield zones map for the study area. The weights determined through AHP calculations were as follows: 38% for GWSA, 24% for rainfall, 4% for drainage density, 7% for the Standard Precipitation Index (SPI), 11% for lineament density, 4% for land use/land cover (LULC), 4% for slope, 4% for lithology, and 4% for aspect (Figure 7). The calculated consistency index (CI) was 0.0286, and using a random consistency index of 1.45 for the nine variables, the resulting consistency ratio was found to be 0.0197, indicating that the assigned weights and the matrix were both significant and coherent.

The analysis of the weighted overlay output indicates that the study area generally has a moderate groundwater yield. Most of the northern region and some parts of the central region exhibit high groundwater yield. In contrast, a considerable portion of the eastern region is characterised by low groundwater yield. An overlay of population points reveals settlements that correspond to the varying groundwater yield zones. Specifically, Local Government Areas (LGAs) that fall within the low groundwater yield zones include Awe and minor parts of Lafia (e.g., Arikya locality), Doma (e.g., Akpanaja locality), and Nasarawa (e.g., Loko locality) (Figure 8). Furthermore, the high groundwater yield zones are Nasarawa Egon, Akwanga, Karu, Wamba, Lafia, and some parts of Obi, Keana, Kokona, Nasara, and Doma.

Table 4: Pairwise comparison matrix of influencing factors

Factors	Drainage Density	Standard Precipitation Index	Lineament	LULC	Slope	Lithology	Aspect	Rainfall	GWSA
Drainage Density	1	0.5	0.33	1	1	1	1	0.2	0.1429
Standard Precipitation Index	2	1	0.5	2	2	2	2	0.25	0.1667
Lineament	3	2	1	3	3	3	3	0.2	0.2
LULC	1	0.5	0.33	1	1	1	1	0.2	0.1429

Slope	1	0.5	0.33	1	1	1	1	0.2	0.1429
Lithology	1	0.5	0.33	1	1	1	1	0.2	0.1429
Aspect	1	0.5	0.33	1	1	1	1	0.2	0.1429
Rainfall	5	4	5	5	5	5	5	1	0.33
GWSA	7	6	5	7	7	7	7	3	1

Table 5: Normalized relative weight of influencing factors

Factors	**Drainage Density**	**Standard Precipitation Index**	**Lineament**	**LULC**	**Slope**	**Lithology**	**Aspect**	**Rainfall**	**GWSA**
Drainage Density	0.05	0.03	0.03	0.05	0.05	0.05	0.05	0.04	0.06
Standard Precipitation Index	0.09	0.06	0.04	0.09	0.09	0.09	0.09	0.05	0.07
Lineament	0.14	0.13	0.08	0.14	0.14	0.14	0.14	0.04	0.08
LULC	0.05	0.03	0.03	0.05	0.05	0.05	0.05	0.04	0.06
Slope	0.05	0.03	0.03	0.05	0.05	0.05	0.05	0.04	0.06
Lithology	0.05	0.03	0.03	0.05	0.05	0.05	0.05	0.04	0.06
Aspect	0.05	0.03	0.03	0.05	0.05	0.05	0.05	0.04	0.06
Rainfall	0.23	0.26	0.38	0.23	0.23	0.23	0.23	0.18	0.14
GWSA	0.32	0.39	0.38	0.32	0.32	0.32	0.32	0.55	0.41

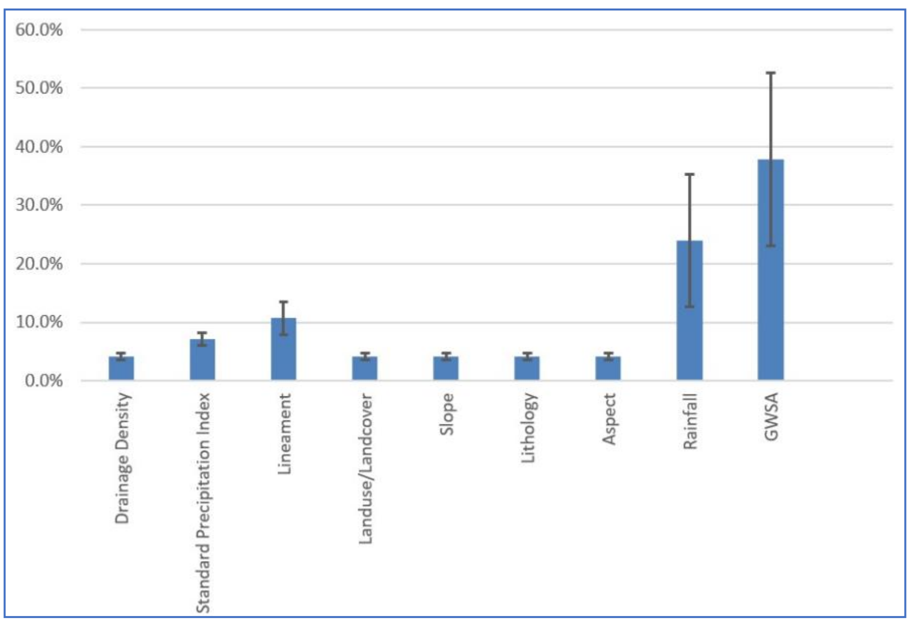

Figure 7: Bar chart showing the percentages assigned to each of the criterion (variables) based on AHP calculations

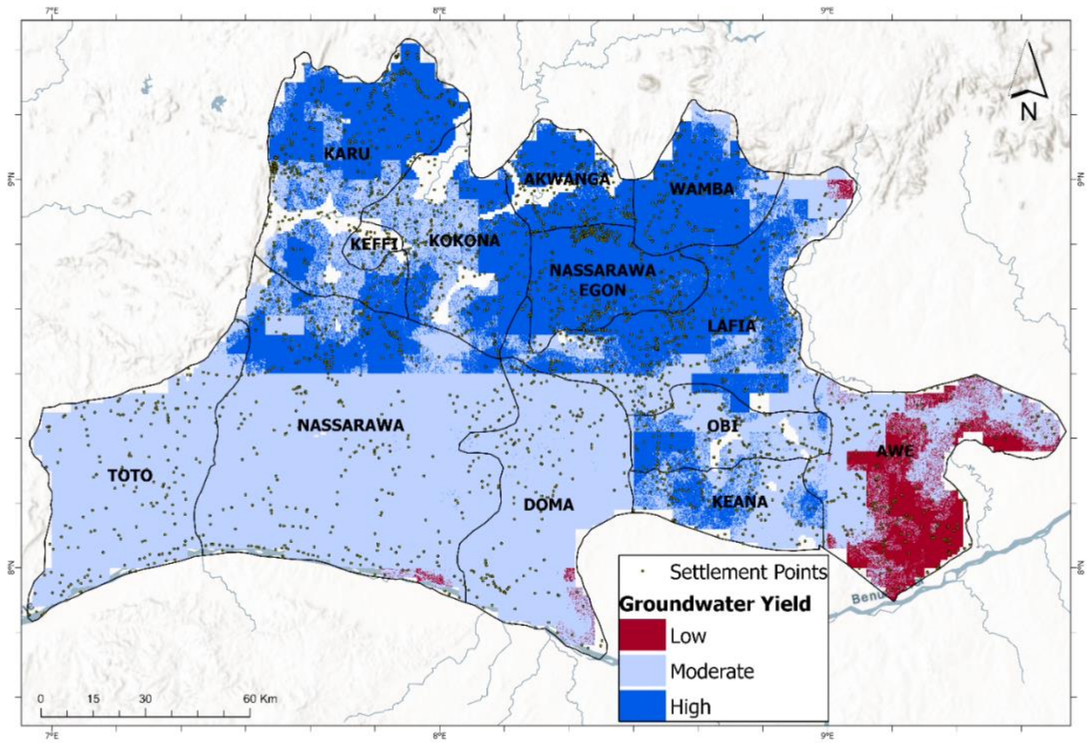

Figure 8: Weighted overlay map from AHP modeling showing low, moderate, and high groundwater yield zones and settlement points that coincide with these zones.

Artificial Intelligence (Machine Learning-Random Forest and Extreme Gradient Boosting)

The results from the Random Forest and XGBoost algorithms are presented in Figures 9, 10, 11, 12a, and b. XGBoost and Random Forest have an overall accuracy of 98% and 99% respectively. The confusion matrices of the models show that both models performed well due to their accurate predictions of the low, moderate, and high groundwater yield classes (Figure 9). A total of 72 and 31 instances of low and moderate groundwater yield were correctly predicted as low and moderate by both models. They both incorrectly classified a moderate instance as low. Random Forest classified all instances correctly as high, while XGBoost classified 4 out of 5 instances as high. Overall, Random Forest performed slightly better than XGBoost in correctly identifying all high groundwater yield zones.

The predicted probability histograms revealed that both models exhibit high confidence levels for a large majority of the test samples (Figure 10). XGBoost shows a slightly higher frequency (100 instances) compared to Random Forest (98 instances). The Precision-Recall (PR) curve shows that the green line (high groundwater yield class) extends from 1.0 (100%) precision horizontally until it reaches and drops down to 100% recall (Figure 11), which indicates that both models performed well in predicting the high groundwater class. Random forest maintained a high precision of 0.76 (76%) for the moderate class (pink line) while XGBoost dropped to 0.4 (40%), which indicates that XGBoost included a higher number of false positives for the moderate class. The Receiver Operating Characteristic (ROC) graph shows that Random Forest demonstrates a superior performance over XGBoost with 100% in all three classes (Figure 12). For example, the graph shows that Random Forest incurred a small false positive rate for the moderate class at 12% while that of XGBoost was 61%.

The XGBoost model assigned the highest feature importance to the SPI (51%) (Figure 13). This is followed by GWSA (18%), rainfall (9%), drainage density (8%), lineament density (7%), lithology (3%), LULC (2%), aspect (2%), and slope (1%). In contrast, the Random Forest model assigned the highest feature importance to the Rainfall (32%) (Figure 14). This is followed by SPI (22%), GWSA (18%), lineament density (10%), drainage density (10%), LULC (3%), slope (2%), lithology (1%), and aspect (1%). The final maps from both models display similar groundwater yield patterns, with few notable differences (Figure 15a and b). Both models agree that Karu, Keffi, and Kokona LGAs are the most dominated by high groundwater yield zones. In contrast, the XGBoost model shows an occurrence of a low groundwater yield pattern in Obi and Keana LGAs (Figure 15a), which is absent in the Random Forest result (Figure 15b).

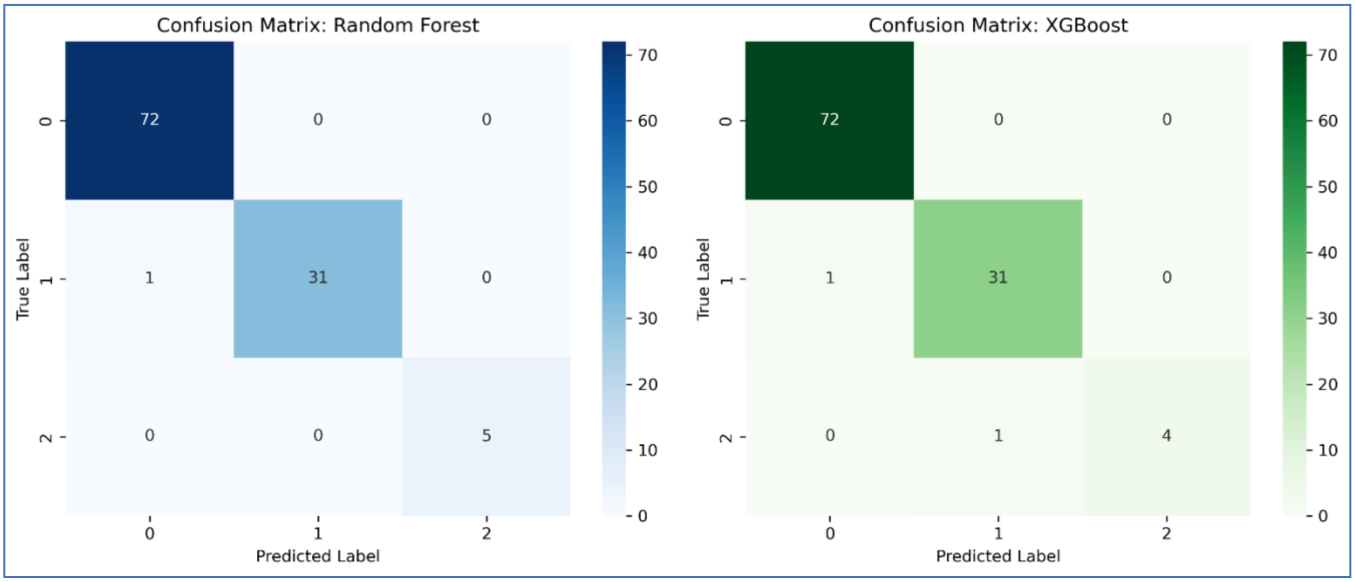

Figure 9: Diagram showing confusion matrices of Random Forest and XGBoost models. Random Forest has a slight edge over XGBoost by correctly predicting all high groundwater yield zones

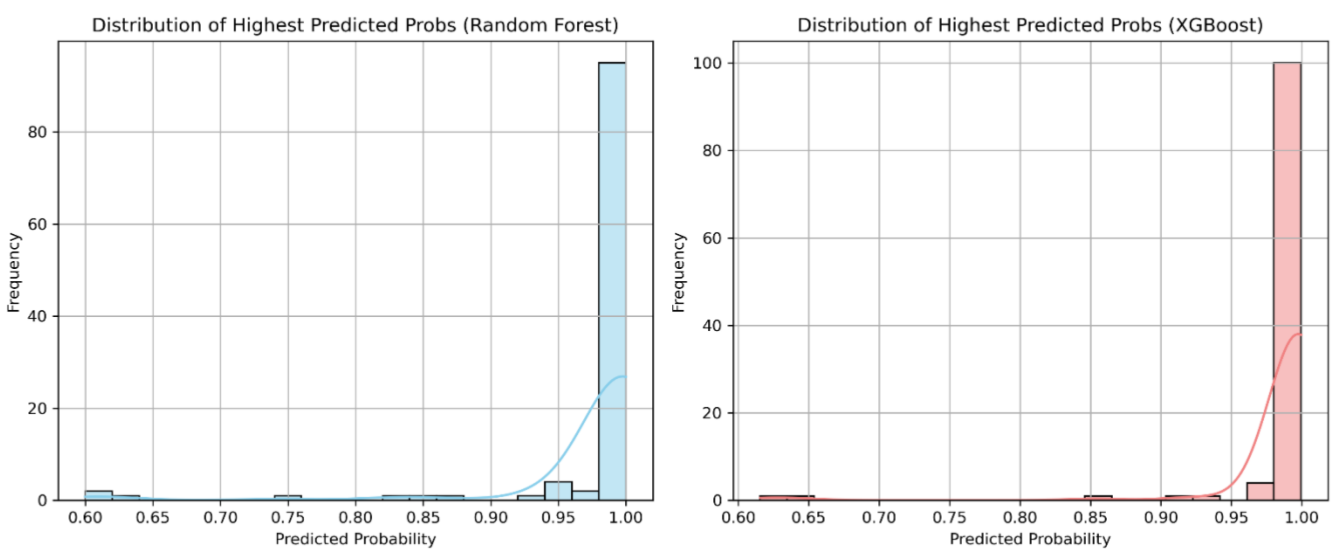

Figure 10: Histogram showing that both Random Forest and XGBoost exhibit a high concentration of predicted probabilities at the maximum confidence (at or close to 100%)

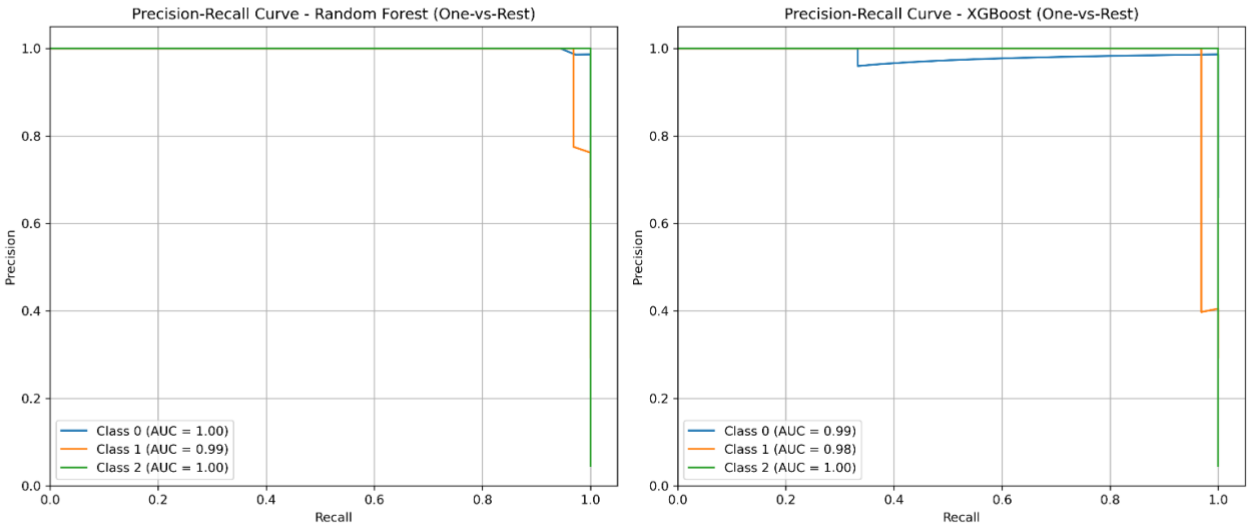

[1]**Figure 11:** Precision-Recall graph showing both Random Forest and XGBoost having high precision and recall with little or no false positives and false negatives in their predictions, respectively

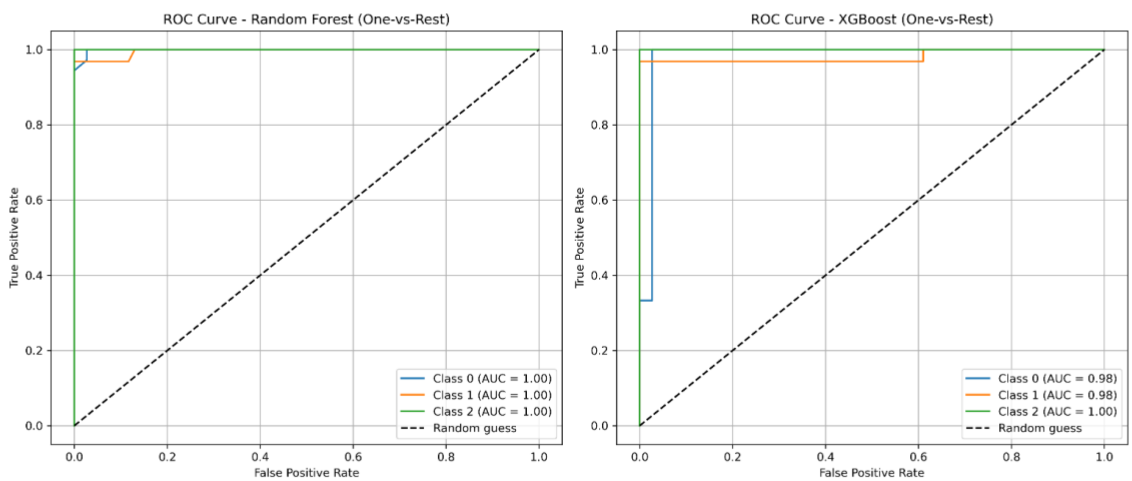

Figure 12: Receiver Operating Characteristic graph showing true positive rate against false positive for both models. The result shows that Random Forest is a better classifier in identifying the different groundwater yield classes

[1]The Class 2 XGBoost curve in Figure 11 appears to have been approximated to 1.00 since it wrongly predicted an instance of high groundwater yield to be moderate yield in the confusion matrix.

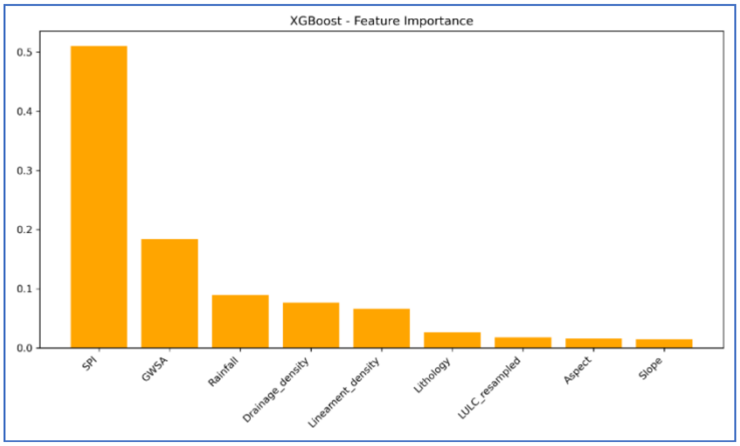

Figure 13: Feature importance from XGBoost modeling indicates SPI to be the most relevant and slope to be the least relevant

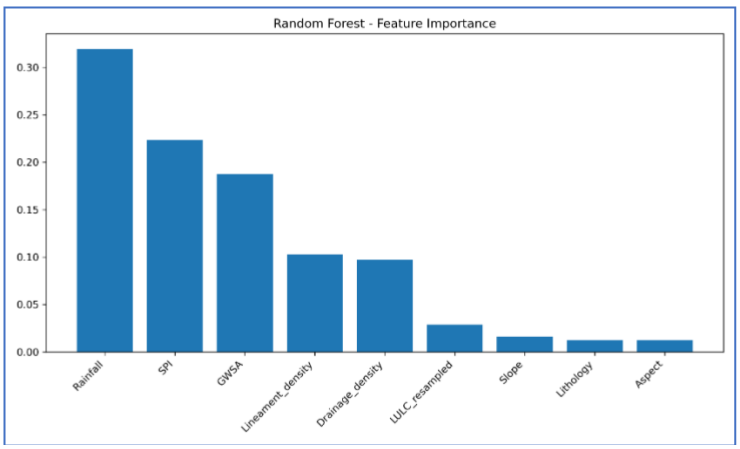

Figure 14: Feature importance from Random Forest modeling indicating Rainfall to be the most relevant and Aspect to be the least relevant

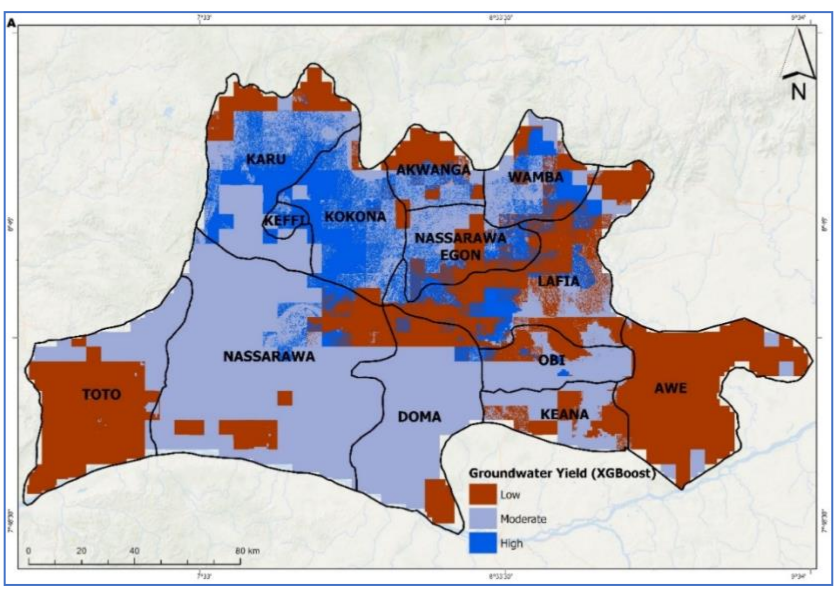

Figure 15a: Map from Extreme gradient (XGBoost) model showing low, moderate, and high groundwater yield patterns

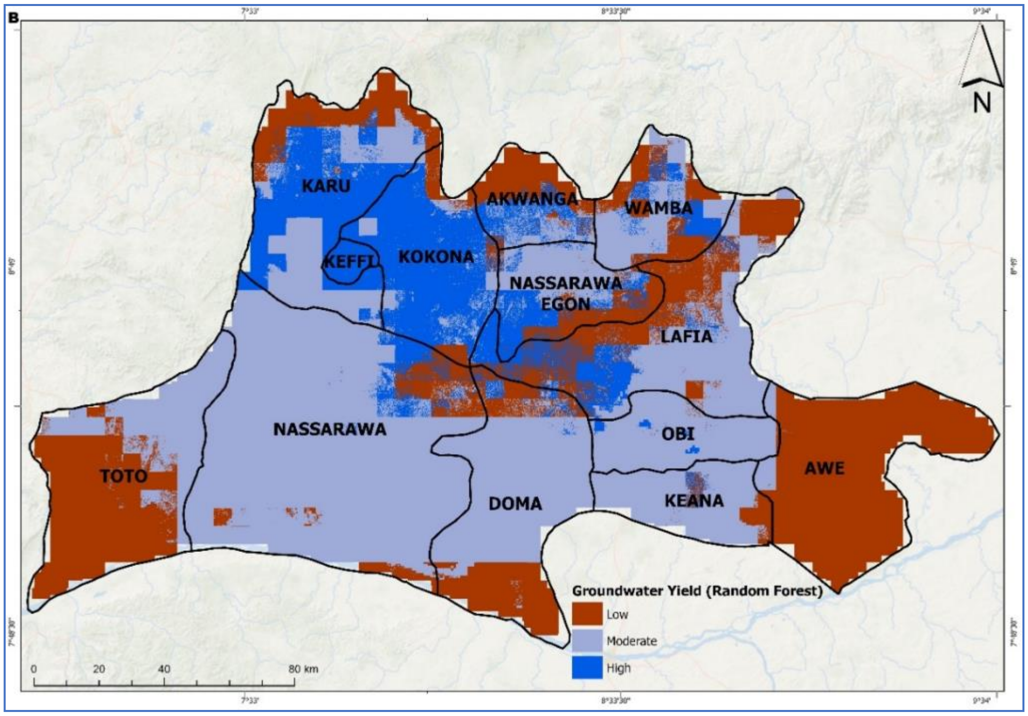

Figure 15b: Map from Random Forest models showing low, moderate, and high groundwater yield patterns. There are a few identifiable differences, some of which include the occurrence of a low groundwater yield pattern in Obi and Keana for the XGBoost result, but absent in the Random Forest result

Discussion and Conclusion

A comprehensive assessment of groundwater yield in the study area was conducted by integrating various geographic parameters for a hybrid approach using the Analytical Hierarchy Process (AHP) and Artificial Intelligence (AI) modeling. This aligns with recent progress in artificial intelligence and the development of hybrid GIS-AI frameworks for intricate hydrogeological mapping, as they offer advantages over traditional single-model approaches (Gacu et al., 2025). This also supports robust decision-making in delineating groundwater yield zones in Nasarawa State, Nigeria.

The slope parameter determines the steepness or gentleness of terrain, which in turn influences the rate of water infiltration into the subsurface. The southern and eastern regions of the study area, characterised by low slope values, indicate high infiltration. While other areas with steep slopes tend to generate greater runoff, resulting in reduced infiltration and diminished groundwater yield (Boitt et al., 2023). These results align with research conducted in the crystalline basement complex of Southwestern Nigeria, showing that slope plays a key role in how groundwater recharge is distributed across the area (Fashae et al., 2013). The lineament structures are also crucial in delineating groundwater yield zones. These structures serve as pathways for groundwater movement. An increase in lineament density results in increased porosity and favorable groundwater prospect zones (Obi Reddy et al., 2000). The orientation of the lineaments to the northeast implies that the overall groundwater flow direction and the structural influences on aquifer systems are also aligned to the northeast. Consequently, zones with elevated lineament density in the southern and central regions are regarded as favorable locations for groundwater storage due to their high infiltration rates (Gupta et al., 2010).

Lithology plays a significant role in determining the porosity and permeability of aquifer rocks (Rahmati et al., 2015). Siliciclastic and unconsolidated lithologies identified in the study area are indicative of the presence of groundwater due to their capacity to facilitate the percolation of surface water (Adelana et al., 2008;

Ige et al., 2021; Ajayi et al., 2022). This supports local hydrogeological studies indicate that the sedimentary formations in the Middle Benue Trough are more productive than the crystalline rocks found in the northern region, which are less permeable (Obrike et al., 2022). Vegetated land plays a crucial role in groundwater recharge by providing pathways for water infiltration, effectively loosening the rock and soil (Shaban et al., 2006). Globally, changes in land use and land cover (LULC) significantly influence groundwater recharge rates (Locke, 2024). Particularly, Forests and vegetation play a crucial role by enhancing natural infiltration processes (Kumari Yadav, 2023; Locke, 2024). Drainage density classification plays a crucial role in understanding the ecosystem of streams and rivers (McManamay & DeRolph, 2019).

Based on the drought analysis and assessment, Nasarawa State has a near-normal drought classification. This result is consistent with Ideki and Nwagbara's (2019) findings, which indicate that Lafia, the state capital of Nasarawa, has a near-normal condition. Additionally, it aligns with Adeaga's (2010) results, which conclude that the Guinea Savanna region in Nigeria typically experiences mild drought. Areas in the eastern and small portions of the north and southwestern areas have regularly experienced drought conditions.

Areas that recorded high rainfall over the past decade are in the northern and central parts of the study area which corroborates the drought results. Some parts of the eastern side (e.g., Lafia and Awe LGAs) and most of the southern part recorded lower rainfall. This indicates that there is a high chance of high groundwater yield in the northern and central parts compared to other parts of the study area.

The qualitative AHP method determined feature importance through pairwise comparisons based on our tacit knowledge of groundwater yield. The results show a general pattern of low, moderate, and high groundwater yield across the study area. The northern and some parts of the central regions were classified as zones of high groundwater yield, while the eastern side was identified as low potential.

Conversely, the AI models (Random Forest and XGBoost) provided more detailed, data-driven results, revealing subtle and distinct patterns that the AHP could not detect. Both models achieved high accuracies of 99% and 98%, respectively, indicating their strong predictive capabilities. XGBoost tends to be more extreme in probability assignment by pushing a slightly higher number of instances to 100% certainty. The high accuracy from the Random Forest analysis in this study align with global standards which shows that ensemble machine learning often surpasses traditional methods when it comes to predicting groundwater occurrences (Feng et al., 2024). The PR and ROC curves demonstrate the superior performance of Random Forest over XGBoost. Although XGBoost performed well, it showed a high false positive rate of 61% for moderate groundwater yield zones and failed to identify some high-yield areas that Random Forest detected. The two models identified different primary drivers of groundwater yield in the study area: XGBoost prioritised SPI at 51%, while Random Forest prioritised rainfall at 32%. This suggests that the internal mechanisms of the models (how their decision trees make predictions) prioritize different geospatial factors. Both models indicates that Karu, Keffi, and Kokona LGAs are the most dominated by high groundwater yield zones while Toto and Awe LGAs are mostly affected by low groundwater yield. The XGBoost model extended the prediction to show an occurrence of low groundwater yield pattern in Obi and Keana LGAs.

In conclusion, AHP provided a foundational framework for evaluating groundwater yield, while AI enhanced the analysis. AI delivered precise, data-validated performance metrics and uncovered complex spatial variations and relationships among features. The AI models, which supported some findings from AHP, identified Keffi, Kokona, the central and southern parts of Karu, the southern part of Akwanga, and Nasarawa Egon as LGAs with high groundwater yield. Conversely, LGAs with low yield include Toto, Awe, the southeastern part of Nasarawa Egon, north of Karu, north of Akwanga, both north and south of Wamba, and the north of Lafia. Identifying low-yield areas provides clear guidance for targeted interventions and adaptive water management strategies to ensure equitable access and sustainable water resource use across the state.

References

Adeaga, O. (2010). Drought risks and impact on water resources in part of northern Nigeria.

https://www.semanticscholar.org/paper/Drought-risks-and-impact-on-water-resources-in-part-Adeaga/717e90e06f5f6d8301ac0b2f571b4e2b0a3896e9.

Adelana, S. M. A., Abiye, T. A., Nkhuwa, D. C. W., Tindinugaya, C., & Oga, M. S. (2008). Urban groundwater management and protection in sub-Saharan Africa. In Adelana, S. M. and MacDonald, A. M. (eds.). Applied groundwater studies in Africa. CRC Press, London, pp. 222–259.

Adesola, G. O., Thamaga, K. H., Gwavava, O., & Pharoe, B. K. (2023). Groundwater Potential Zones Assessment Using Geospatial Models in Semi-Arid Areas of South Africa. *Land*, 12(10), 1877. https://doi.org/10.3390/land12101877.

Adewumi, T., & Salako, K. (2017). Delineation of mineral potential zone using high resolution aeromagnetic data over part of Nasarawa State, North Central, Nigeria. *Egyptian Journal of Petroleum,* pp. 27. 10.1016/j.ejpe.2017.11.002.

Afan, H. A., Osman, A. I. A., Essam, Y., Ahmed, A. N., Huang, Y. F., Kisi, O., Sherif, M., Sefelnasr, A., Chau, K.-W., & El-Shafie, A. (2021). Modeling the fluctuations of groundwater level by employing ensemble deep learning techniques. *Engineering Applications of Computational Fluid Mechanics*. 15, 1420–1439.

Ahmed, A., Ranasinghe-Arachchilage, C., Alrajhi, A., & Hewa, G. (2021). Comparison of multicriteria decision-making techniques for groundwater recharge potential zonation: Case study of the Willochra Basin, South Australia. *Water*, 13(4), Article 525. https://doi.org/10.3390/w13040525.

Ajayi G. O., Ifeanyi, J. N., Joseph, O. O., Oluwatobi, O. A., & Ishola, O. A. (2022). Assessment and delineation of groundwater potential zones using integrated geospatial techniques and analytic hierarchy process. *Applied Water Science*, 12, 276 https://doi.org/10.1007/s13201-022-01802-4.

Alam, A., Rahman, M. S., Saadat, A. H. M., & Huq, M. M. (2012). Gamma distribution and its application of spatially monitoring meteorological drought in Barind, Bangladesh. *Journal of Environmental Science and Natural Resources,* 5(2). https://doi.org/10.3329/jesnr.v5i2.14832.

Alao, J. O., Lawal, H. A., Abubakar, F., & Abdulsalami, M. (2024). Geophysical and physicochemical assessment of groundwater and the implication on the public health in rural and semi-urban areas of Northern Nigeria. *Discover Environment*, 2(44), 1, 00079-y.

Ayodele-Olajire, D. O. (2022). Power in water governance: the case of Prescott Active Management Area, Arizona. *GeoJournal*, 87(3), 1983-1999. doi.org/10.1007/s10708-020-10344-8.

Ayodele-Olajire, D. O., & Bolin, B. (2019). Achieving Water Sustainability through Coordination among Stakeholders. *Yearbook of the Association of Pacific Coast Geographers*, 81, 135-157.

Ayodele-Olajire, D., & Olusola, A. (2022). A review of climate change trends and scenarios (2011–2021). *Current Directions in Water Scarcity Research*, 7, 545-560. doi.org/10.1016/B978-0-323-91910-4.00031-5.

Boitt, M., Khayasi, P., & Wambua, C. (2023). Assessment of groundwater potential and prediction of the potential trend up to 2042 using GIS-Based model and remote sensing techniques for Kiambu County. *International Journal of Geosciences,* 14(10), 951-974. 1https://doi.org/10.4236/ijg.2023.1410053.

Bordi, I., Fraedrich, K., Petitta, M., & Sutera, A. (2007). Extreme value analysis of wet and dry periods in Sicily. *Theoretical and Applied Climatology,* 87, 61-71. 10.1007/s00704-005-0195-3.

Cardiff University. (n.d.). RIGSS: Field Summary Lafia and Nasarawa State. Retrieved fromhttps://www.cardiff.ac.uk/__data/assets/pdf_file/0013/1211314/Lafia_summary.pdf.

Chen, S.-T., Kuo, Chun-Chao, & Yu, P.-S. (2009). Historical trends and variability of meteorological droughts in Taiwan. *Hydrological Sciences Journal,* 54(3), 430–441. https://doi.org/10.1623/hysj.54.3.430.

Ezekiel, A., & Dominic, A. A. (2015). Sources, demand and problems of domestic water in

Nassarawa Eggon Town, Nigeria. *Pollution,* 1(1), 55-65. 10.7508/pj.2015.01.006.

Fashae, Olutoyin., Tijani, Moshood., Tijani, Talabi, Abel, & Oluwatola, Adedeji (2013). Delineation of groundwater potential zones in the crystalline basement terrain of SW-Nigeria: an integrated GIS and remote sensing approach. *Journal of applied water science,* 10.1007/s13201-013-0127-9.

Feng, F., Ghorbani, H., & Radwan, A. E. (2024). Predicting groundwater level using traditional and deep machine learning algorithms. *Frontiers in Environmental Science*, 12, 1291327. https://doi.org/10.3389/fenvs.2024.1291327.

Fenta, A. A., Kifle, A., Gebreyohannes, T., & Hailu, G. (2015). Spatial analysis of groundwater potential using remote sensing and GIS-based multi-criteria evaluation in RayaValley, northern Ethiopia. *Hydrogeology Journal, 23,* 195–206.

Gacu, J. G., Monjardin, C. E. F., Mangulabnan, R. G. T., & Mendez, J. C. F. (2025). Application of Artificial Intelligence in Hydrological Modeling for Streamflow Prediction in Ungauged Watersheds: A Review. *Water*, 17(18), 2722. https://doi.org/10.3390/w17182722.

Gerlach, M. E., Rains, K. C., Guerrón-Orejuela, E. J., Kleindl, W. J., Downs, J., Landry, S. M., & Rains, M. C. (2022). Using remote sensing and machine learning to locate groundwater discharge to salmon-bearing streams. *Remote Sensing*, 14(1), 63. https://doi.org/10.3390/rs14010063.

Gupta, M., & Srivastava, P. K. (2010). Integrating GIS and remote sensing for identification of groundwater yield zones in the hilly terrain of Pavagarh, Gujarat, India. *Water International*. 35(2), 233– 245. doi:10.1080/02508061003664419.

Ideki, O., & Nwagbara, M. O. (2019). Geo-Spatial Assessment of Vegetation Response to Drought in North Central Nigeria. *Journal of Geoscience and Environment Protection,* 7(3), Article 3. https://doi.org/10.4236/gep.2019.73003.

Idowu, I. O., & Ojo, A. O. (2024). Exploring groundwater resources in southwestern Nigeria: An integrated geophysical approach. *Hydrology Research*, 7(3). https://doi.org/10.1016/j.hydres.2024.04.002.

Ifediegwu, S. I. (2022). Assessment of groundwater potential zones using GIS and AHP techniques: a case study of the Lafia district, Nasarawa State, Nigeria. *Applied Water Science,* 12, 10. https://doi.org/10.1007/s13201-021-01556-5.

Ige, O. O., Ameh, H. O., & Olaleye, I. M. (2021). Borehole inventory, groundwater potential and water quality studies in Ayede Ekiti, Southwestern Nigeria. *Discover Water,* 1, 2. https://doi. org/ 10.1007/s43832-020- 00001-z.

Igwe, O., Ifediegwu, S. I., & Onwuka, O. S. (2020). Determining the occurrence of potential groundwater zones using integrated hydrogeomorphic parameters, GIS and remote sensing in Enugu State, Southeastern. *Nigeria Sustainable Water Resource Management,* 6, 39. https://doi. org/ 10. 1007/ s40899- 020-00397-5.

Iloeje, N. P. (1981). A new geography of Nigeria. New, revised. Longman Publishers, London.

Kana, M. A., Schoeneich, K., & Garba, M. L. (2014). Water supply situation in the crystalline hydrogeological province of Northern Nigeria: A case study of Nasarawa Town and Environs, Northcentral Nigeria. *American International Journal of Contemporary Research*, 4(11), 160. https://www.aijcrnet.com/journals/Vol_4_No_11_November_2014/13.pdf.

Kordestani, M. D., Naghibi, S. A., Hashemi, H., Ahmadi, K., Kalantar, B., & Pradhan, B. (2019). Groundwater potential mapping using a novel data-mining ensemble model. *Hydrogeology Journal,* 27, 211–224. https://doi. org/ 10. 1007/ s10040- 018-1848-5.

Kumari, Yadav S. (2023). Land Cover Change and Its Impact on Groundwater Resources: Findings and Recommendations. Groundwater - *New Advances and Challenges. IntechOpen*. https://doi.org/10.5772/intechopen.110311.

Lavanya, M., & Muthukumar, M. (2024). AHP and geospatial technologies for identifying groundwater exploration target regions in Dindigul, southern India. *Geosystems and Geoenvironment,* 3(4), 100315. https://doi.org/10.1016/j.geogeo.2024.100315.

Locke, K. (2024). Impacts of land use/land cover on water quality: A contemporary review for researchers and policymakers. *Water Quality Research Journal,* 59, 89-106. 10.2166/wqrj.2024.002.

Ma, Y., Pan, Y., Zhang, C., Yeh, F., Xu, L., Huang, Z., & Gong, H. (2024). Improved Estimates of Sub-Regional Groundwater Storage Anomaly Using Coordinated Forward Modeling. *Water Resources Research*, 60(7), e2023WR036105. https://doi.org/10.1029/2023WR036105.

MacDonald, G. (2010). Water, climate change, and sustainability in the southwest. *Proceedings of the National Academy of Sciences*, 107(50), 21256–21262. https://doi.org/10.1073/pnas.1007326107.

McManamay, R. A., & DeRolph, C. R. (2019). A Stream Classification System for the Conterminous United States. *Scientific Data,* pp. 6. *190017*.https://doi.org/10.1038/sdata.2019.17.

Morea, H., & Samanta, S. (2020). Multi-criteria decision approach to identify flood vulnerability zones using geospatial technology in the Kemp-Welch Catchment, Central Province, Papua New Guinea. *Applied Geomatics*, 12(4), 427–440. https://doi.org/10.1007/s12518-020-00315-6.

Muralitharan, J., & Palanivel, K. (2015). Groundwater targeting using remote sensing, geographical information system and analytical hierarchy process method in hard rock aquifer system, Karur district, Tamil Nadu, India. *Earth Science Informatics,* 8(4), 827–842. doi:10.1007/s12145-015-0213-7.

Nishimura, R., Jones, N. L., Williams, G. P., Ames, D. P., Mamane, B., & Begou, J. (2022). Methods for Characterizing Groundwater Resources with Sparse in Situ Data. *Hydrology*, 9(8), 134. https://doi.org/10.3390/hydrology9080134.

Obaje, D. O., Yahaya, M., & Shammah, E. C. (2020). Quality of groundwater sources in Keffi and Karu Local Government Areas, Nigeria. *International Journal of Advanced Academic Research,* 6(2), 156-166.

Obateru, R., Adeyefa, A., & Fashae, O. A. (2023). Drought assessment and rainfall trend analysis in southwestern Nigeria. *World Water Policy*, 9(2), 254–273. https://doi.org/10.1002/wwp2.12102.

Obi, R. G. P., Chandra, M. K., Srivastav, S. K., Srinivas, C. V., & Maji, A. K. (2000). Evaluation of groundwater potential zones using remote sensing data a case study of Gaimukh watershed. Bhandara district, Maharashtra. *Journal of the Indian Society of Remote Sensing*, 28(1), 19–32.

Obrike, S., Baba Oleka, Adama, B. S., Ojuola, Anudu, Goodluck, Abdulahi, Kana, Iliya, & Mamidak (2022). Hydro-geophysical assessment of groundwater potential and aquifer vulnerability of the Turonian Makurdi Formation in North-Bank area, Makurdi, middle Benue Trough, Nigeria. *Journal of Mining and Geology,* 58, 189-201.

Ogunrinde, A. T., Oguntunde, P. G., Akinwumiju, A. S., & Fasinmirin, J. T. (2019). Analysis of recent changes in rainfall and drought indices in Nigeria, 1981–2015. *Hydrological Sciences Journal,* 64(14), 1755–1768. https://doi.org/10.1080/02626667.2019.1673396.

Olabode, O. F., Adebayo, A. D., & Ekundayo, O. Y. (2021). Drought analysis and groundwater prioritization of a typical data-scarce drought-prone hydrological basin using geospatial techniques. *Groundwater for Sustainable Development,* 13, 100581. https://doi.org/10.1016/j.gsd.2021.100581.

Olden, J. D., Lawler, J. J., & Poff, N. L. (2008). Machine Learning Methods Without Tears: A Primer for Ecologists. *The Quarterly Review of Biology,* https://doi.org/10.1086/587826.

Oni, A. G., Eniola, P. J., Olorunfemi, M. O., Okunubi, M. O., & Osotuyi, G. A. (2020). The magnetic method as a tool in groundwater investigation in a basement complex terrain: Modomo Southwest Nigeria as a case study. *Applied Water Science,* 10(8), 190. https://doi.org/10.1007/s13201-020-01279-z.

Orimoloye, Israel, Zhou, Leocadia & Kalumba, Ahmed Mukalazi (2021). Drought Disaster Risk Adaptation through Ecosystem Services-Based Solutions: Way Forward for South Africa. *Sustainability.* 13, 4132. 10.3390/su13084132.

Oseji, J., & Ofomola, M. (2010). Determination of groundwater flow direction in Utagba Ogbe Kingdom, Udukwa Land Area of Delta State, Nigeria. *Journal of Earth Science,* 4(1), 32–34.

Pradhan, B. (2009). Groundwater potential zonation for basaltic watersheds using satellite remote sensing data and GIS techniques. *Central European Journal of Geosciences,* 1(1), 120–129. doi:10.2478/v10085-009-0008-5.

Rahmati, O., Nazari Samani, A., Mahdavi, M., Pourghasemi, H. R., & Zeinivand, H. (2015). Groundwater yield mapping at Kurdistan region of Iran using analytic hierarchy process and GIS. *Arabian Journal of Geosciences*, 8(9), 7059–7071. doi:10.1007/s12517-014-1668-4.

Ren, X., Li, P., Wang, D., Zhang, Q., & Ning, J. (2024). Drivers and characteristics of groundwater drought under human interventions in arid and semiarid areas of China. *Journal of Hydrology*, 631, 130839.

Rodell, M., & Reager, J. T. (2023). Water cycle science enabled by the GRACE and GRACE-FO satellite missions. *Nature Water,* 1(1), 47–59. https://doi.org/10.1038/s44221-022-00005-0.

Saaty, T. L. (1980). The analytic hierarchy process (AHP). *The Journal of the Operational Research Society*, 41(11), 1073-1076.

Saaty, T. L. (1990). How to make a decision: the analytic hierarchy process. *European journal of operational research*, 48(1), 9-26.

Shaban, A., Khawlie, M., & Abdallah, C. (2006). Use of remote sensing and GIS to determine recharge yield zones: The case of Occidental Lebanon. *Hydrogeology Journal*, 14(4), 433–443. doi:10.1007/s10040-005-0437-6.

Sordo-Ward, A., Bejarano, M. D., Iglesias, A., Asenjo, V., & Garrote, L. (2017). Analysis of Current and Future SPEI Droughts in the La Plata Basin Based on Results from the Regional Eta Climate Model. *Water,* 9(11), Article 11. https://doi.org/10.3390/w9110857.

Svoboda, Mark, Hayes, Michael & Wood, Deborah (2012). Standardized Precipitation Index: User Guide.

Tanriverdi, I., & Batmaz, İ. (2025). AI-driven U.S. drought prediction using machine learning and deep learning. Climate Dynamics, 63, 249. https://doi.org/10.1007/s00382-025-07720-w.

Thapa, R., Gupta, S., Guin, S., & Kaur, H. (2017). Assessment of groundwater potential zones using multi-influencing factor (MIF) and GIS: a case study from Birbhum district, West Bengal. *Applied Water Science,* 7(9), 1–15.

Todd, D. K. (2004). *Ground Water Hydrology*. John Wiley & Sons, New York.

Wang, J., Chakraborty, C., & Ouyang, H. (2008). The Analytic Hierarchy Process: Structuring, Measurement, and Synthesis. *Encyclopedia of decision making and decision support technologies,* pp. 29-37. IGI Global.

Yıldırım, Ü. (2021). Identification of groundwater potential zones using GIS and multi-criteria decision-making techniques: a case study upper Coruh River basin (NE Turkey). ISPRS.

Zaresefat, M., Derakhshani, R., Nikpeyman, V., GhasemiNejad, A., & Raoof, A. (2022). Using Artificial Intelligence to Identify Suitable Artificial Groundwater Recharge Areas for the Iranshahr Basin. *Water,* 15(6), 1182. https://doi.org/10.3390/w15061182.